PAPER

Frequency-Domain Space-Time Block Coded-Joint Transmit/Receive Diversity for Direct-Sequence Spread Spectrum Signal Transmission

Hiromichi TOMEBA[†a)], **Kazuaki TAKEDA**[†], ***Student Members***, ***and*** **Fumiyuki ADACHI**[†], ***Member***

SUMMARY Recently, we proposed space-time block coded-joint transmit/receive antenna diversity (STBC-JTRD) for narrow band transmission in a frequency-nonselective fading channel; it allows an arbitrary number of transmit antennas while limiting the number of receive antennas to 4. In this paper, we extend STBC-JTRD to the case of frequency-selective fading channels and propose frequency-domain STBC-JTRD for broadband direct sequence-spread spectrum (DSSS) signal transmission. A conditional bit error rate (BER) analysis is presented. The average BER performance in a frequency-selective Rayleigh fading is evaluated by Monte-Carlo numerical computation method using the derived conditional BER and is confirmed by computer simulation of the signal transmission. Performance comparison between frequency-domain STBC-JTRD transmission and joint space-time transmit diversity (STTD) and frequency-domain equalization (FDE) reception is also presented.

key words: *frequency-selective fading channel, frequency-domain pre-equalization, space-time block coding, transmit/receive antenna diversity, DSSS*

1. Introduction

High speed data transmissions of over 100 Mbps are required for the next generation mobile communications systems. However, the mobile channel is composed of many propagation paths with different time delays, producing a severe frequency-selective fading channel, and therefore, the bit error rate (BER) performance significantly degrades due to a severe inter-symbol interference (ISI) [1]–[3]. Frequency-domain equalization (FDE) is an effective technique for improving the single-carrier (SC) transmission performance in a frequency-selective fading channel [4]. FDE can be applied to direct-sequence code division multiple access (DS-CDMA) to obtain a good BER performance similar to that of multi-carrier CDMA (MC-CDMA) [5], [6].

Another promising equalization technique is the frequency-domain pre-equalization (pre-FDE) transmission [7]–[9]. Recently, we had proposed pre-FDE for DS-CDMA and showed that it can achieve a good BER performance similar to FDE reception in a frequency-selective fading channel [10]. By using pre-FDE transmission and FDE reception, all the frequency-domain equalization processing can be implemented at only one transceiver side [10] (For performing pre-FDE, the channel state information (CSI) is necessary at the transmitter side. In a mobile communication system using time division duplex (TDD) [11], the CSI can be estimated using the received signal since the same carrier frequency is used for both transmit and receive channels.)

To further improve the DS-CDMA transmission performance, the antenna diversity technique can be used [1]–[3]. Joint pre-FDE and transmit antenna diversity was proposed in [9], [10]. However, the use of antenna diversity reception for a pre-FDE transmission system is not straightforward since the signals received at different receive antennas cannot be coherently combined by using complex transmit weights only. To the best of authors' knowledge, there has been no literature available for joint use of pre-FDE transmission and antenna diversity reception. Recently, we proposed the space-time block coded-joint transmit/receive diversity (STBC-JTRD) for narrow-band SC transmission in a frequency-nonselective fading channel [12], [13]. An arbitrary number of transmit antennas can be used while the number of receive antennas is limited to 4. It should be noted that STBC-JTRD can achieve the receive antenna diversity gain without requiring the CSI at the receiver side. In this paper, we extend the STBC-JTRD [12], [13] to the case of frequency-selective fading channel and propose a frequency-domain STBC-JTRD for broadband direct-sequence spread spectrum (DSSS) transmission.

The remainder of this paper is organized as follows. Section 2 introduces the principle of STBC-JTRD encoding/decoding. Section 3 describes the frequency-domain STBC-JTRD for DSSS. The pre-equalization weight based on minimum mean square error (MMSE) criterion is derived in Sect. 4. The conditional BER analysis is presented in Sect. 5. In Sect. 6, the average BER performance is numerically evaluated by Monte-Carlo numerical computation method using the derived conditional BER and is confirmed by computer simulation of the signal transmission. Section 7 offers some conclusions.

2. STBC-JTRD Encoding/Decoding Principle

STBC-JTRD encoding [13] is illustrated in Fig. 1. An information symbol sequence $\{d_j\}$ to be transmitted is grouped into a sequence of blocks of J symbols each. Each block

Manuscript received April 12, 2006.
Manuscript revised October 17, 2006.

[†]The authors are with the Dept. of Electrical and Communication Engineering, Graduate School of Engineering, Tohoku University, Sendai-shi, 980-8579 Japan.
a) E-mail: tomeba@mobile.ecei.tohoku.ac.jp

DOI: 10.1093/ietcom/e90–b.3.597

is encoded into N_t parallel codewords; each codeword consists of Q symbols and is transmitted from one of the N_t transmit antennas. A combination of J and Q is shown in Table 1 for a number N_r 1–4 of receive antennas. As discussed in [13], the signals to be transmitted from N_t transmit antennas are multiplied by the corresponding complex transmit weights to achieve a diversity gain similart to N_r-branch maximal ratio combining (MRC) receive diversity by performing STBC-JTRD decoding at the receiver. However, since the noise power after STBC-JTRD decoding is increased by N_r times compared to $N_t \times N_r$-branch MRC receive diversity, the diversity gain is reduced by $10 \log N_r$ (dB) from $N_t \times N_r$-branch MRC receive diversity. The STBC-JTRD decoding requires the addition/subtraction and conjugate operations, but requires no channel state information (CSI).

As an example, $N_r = 2$, we have $J = Q = 2$ and STBC-JTRD encoding is expressed as [13]

$$\begin{pmatrix} s_{0,n} \\ s_{1,n} \end{pmatrix} = \left(\sum_{n=0}^{N_t-1} \sum_{m=0}^{1} |h_{m,n,0}|^2 \right)^{-1/2} \begin{pmatrix} d_0 h^*_{0,n,0} + d_1 h^*_{1,n,0} \\ d^*_0 h^*_{1,n,0} - d^*_1 h^*_{0,n,0} \end{pmatrix}, \quad (1)$$

where $s_{q,n}$ is the coded symbol to be transmitted from the n-th transmit antenna in the q-th time slot (q=0, 1) and $h_{m,n,0}$ is the complex channel path gain between the n-th transmit antenna and the m-th receive antenna. STBC-JTRD decoding to get the decision variable $\hat{d}_j$, j=0, 1, is represented as

$$\begin{pmatrix} \hat{d}_0 \\ \hat{d}_1 \end{pmatrix} = \begin{pmatrix} r_{0,0} + r^*_{1,1} \\ r_{0,1} - r^*_{1,0} \end{pmatrix}, \quad (2)$$

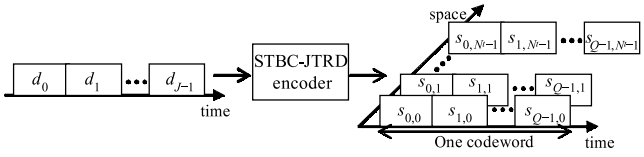

Fig. 1 STBC-JTRD encoding.

Table 1 J, Q and R for N_r=2–4.

No. of receive antennas, N_r	No. of information symbol blocks in a codeword, J	No. of coded symbol blocks in a codeword, Q	Coding rate, R
1	1	1	1
2	2	2	1
3	3	4	3/4
4	3	4	3/4

where $r_{q,m}$ is the q-th received symbol in a codeword received by the m-th receive antenna.

3. Frequency-Domain STBC-JTRD for DSSS

Figure 2 illustrates the transmitter/receiver structure for DSSS using frequency-domain STBC-JTRD. Throughout the paper, chip-spaced discrete time representation of the transmitted signal is used. In what follows, without loss of generality, we assume the transmission of one codeword (transmission of JN_c/SF data symbols $\{d(i); i=0\sim(J(N_c/SF)-1)\}$).

3.1 Frequency-Domain STBC-JTRD Encoding

At the transmitter, a sequence of data modulated symbols $\{d(i)\}$ is spread using a complex spreading code $\{c(u); u=0\sim(JN_c-1)\}$ with $|c(u)|=1$ having the spreading factor SF. The resultant DSSS signal is divided into a sequence of blocks of N_c chips each. The j-th chip block $\{s_j(t); t=0\sim(N_c-1)\}$ is expressed, using the equivalent low-pass representation, as

$$s_j(t) = c(t + jN_c) d\left(\left\lfloor \frac{t + jN_c}{SF} \right\rfloor \right), \quad (3)$$

where $\lfloor x \rfloor$ is the largest integer smaller than or equal to x. N_c-point fast Fourier transform (FFT) is applied to decompose the j-th chip block into N_c frequency components $\{S_j(k); k=0\sim(N_c-1)\}$ as

$$S_j(k) = \sum_{t=0}^{N_c-1} s_j(t) \exp\left(-j2\pi t \frac{k}{N_c} \right). \quad (4)$$

The J consecutive k-th frequency components $\{S_j(k); j=0\sim(J-1)\}$ is encoded into N_t parallel codewords. The n-th parallel codeword ($n=0\sim(N_t-1)$) is composed of Q consecutive blocks $\{\tilde{S}_{q,n}(k); q=0\sim(Q-1)\}$ for the transmission from the n-th transmit antenna.

When N_r=1, an information symbol block is encoded into a codeword $\{\tilde{S}_{0,n}(k)\}$, $n=0\sim(N_t-1)$, as

$$\tilde{S}_{0,n}(k) = C_1 S_0(k) w^*_{0,n}(k) \quad \text{for } N_r = 1. \quad (5a)$$

When N_r=2, the J=2 information symbol blocks are encoded into two codewords, each consisting of Q=2 consecutive blocks $\{\tilde{S}_{0,n}(k), \tilde{S}_{1,n}(k)\}$, $n=0\sim(N_t-1)$, as

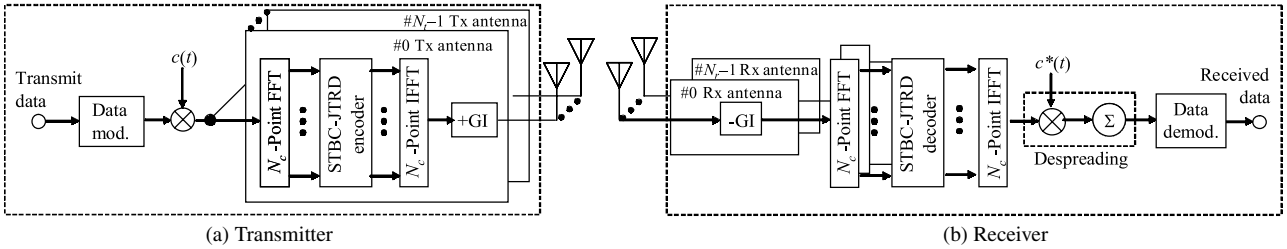

(a) Transmitter (b) Receiver

Fig. 2 Transmitter/receiver structure for DSSS with frequency-domain STBC-JTRD.

$$\begin{pmatrix} \tilde{S}_{0,n}(k) \\ \tilde{S}_{1,n}(k) \end{pmatrix} = C_2 \begin{pmatrix} S_0(k)w^*_{0,n}(k) + S_1(k)w^*_{1,n}(k) \\ S^*_0(k)w^*_{1,n}(k) - S^*_1(k)w^*_{0,n}(k) \end{pmatrix} \quad \text{for} \quad N_r = 2. \tag{5b}$$

When N_r=3 and 4, the J=3 information symbol blocks are encoded into four codewords, each consisting of Q=4 consecutive blocks $\{\tilde{S}_{q,n}(k);\ q{=}0{\sim}3\}$, $n{=}0{\sim}(N_t-1)$, as

$$\begin{pmatrix} \tilde{S}_{0,n}(k) \\ \tilde{S}_{1,n}(k) \\ \tilde{S}_{2,n}(k) \\ \tilde{S}_{3,n}(k) \end{pmatrix} = C_3 \begin{pmatrix} S_0(k)w^*_{0,n}(k) + S_1(k)w^*_{1,n}(k) + S_2(k)w^*_{2,n}(k) \\ S^*_0(k)w^*_{1,n}(k) - S^*_1(k)w^*_{0,n}(k) \\ S^*_0(k)w^*_{2,n}(k) - S^*_2(k)w^*_{0,n}(k) \\ S^*_1(k)w^*_{2,n}(k) - S^*_2(k)w^*_{1,n}(k) \end{pmatrix} \quad \text{for} \quad N_r = 3, \tag{5c}$$

$$\begin{pmatrix} \tilde{S}_{0,n}(k) \\ \tilde{S}_{1,n}(k) \\ \tilde{S}_{2,n}(k) \\ \tilde{S}_{3,n}(k) \end{pmatrix} = C_4 \begin{pmatrix} S_0(k)w^*_{0,n}(k) + S_1(k)w^*_{1,n}(k) + S_2(k)w^*_{2,n}(k) \\ S^*_0(k)w^*_{1,n}(k) - S^*_1(k)w^*_{0,n}(k) + S_2(k)w^*_{3,n}(k) \\ S^*_0(k)w^*_{2,n}(k) - S_1(k)w^*_{3,n}(k) - S^*_2(k)w^*_{0,n}(k) \\ S_0(k)w^*_{3,n}(k) + S^*_1(k)w^*_{2,n}(k) - S^*_2(k)w^*_{1,n}(k) \end{pmatrix} \quad \text{for } N_r = 4. \tag{5d}$$

In Eq. (5), $w_{m,n}(k)$, $m{=}0{\sim}(N_r-1)$ and $n{=}0{\sim}(N_t-1)$, is the MMSE pre-equalization weight, which will be derived in Sect. 4. C_{N_r} is the power normalization factor, given by

$$C_{N_r} = \sqrt{\frac{N_c}{\sum_{m=0}^{N_r-1}\sum_{n=0}^{N_t-1}\sum_{k=0}^{N_c-1}|w_{m,n}(k)|^2}}, \tag{6}$$

which acts as transmit power control factor.

After STBC-JTRD encoding, N_c-point IFFT is applied to each one of the N_t codewords to generate the N_t time-domain DSSS signal blocks. The q-th time-domain DSSS signal block $\{\tilde{s}_{q,n}(t);\ t{=}0{\sim}(N_c-1)\}$, to be transmitted from the n-th transmit antenna $n{=}0{\sim}(N_t-1)$, is given by

$$\tilde{s}_{q,n}(t) = \sqrt{\frac{2E_c}{T_c}} \left\{ \frac{1}{N_c} \sum_{k=0}^{N_c-1} \tilde{S}_{q,n}(k) \exp\left(j2\pi k \frac{t}{N_c}\right) \right\}, \tag{7}$$

where E_c and T_c denote the transmit chip energy and the chip period, respectively. After inserting a cyclic prefix of N_g chips into the guard interval (GI), N_t DSSS signal blocks of (N_c+N_g) chips each are transmitted from all the N_t transmit antennas.

3.2 Frequency-Domain STBC-JTRD Decoding

A superposition of N_t transmitted signal blocks is received via a frequency-selective fading channel at N_r receive antennas. We assume a chip-spaced L-path frequency-selective block fading channel. The channel impulse response $h_{m,n}(\tau)$ is expressed as

$$h_{m,n}(\tau) = \sum_{l=0}^{L-1} h_{m,n,l}\delta(\tau - \tau_l), \tag{8}$$

where $h_{m,n,l}$ and τ_l are the complex-valued path gain and time delay of the l-th propagation path between the n-th transmit antenna and the m-th receive antenna. The q-th block $r_{q,m}(t)$, in a codeword, received by the m-th receive antenna, can be expressed as

$$r_{q,m}(t) = \sum_{n=0}^{N_t-1}\sum_{l=0}^{L-1} h_{m,n,l}\tilde{s}_{q,n}(t-\tau_l) + \eta_{q,m}(t), \tag{9}$$

where $\eta_{q,m}(t)$ is the additive white Gaussian noise (AWGN) process with a zero mean and a variance $2N_0/T_c$ with N_0 being the single-sided power spectrum density.

After the removal of the GI, $\{r_{q,m}(t);\ t{=}0{\sim}(N_c-1)\}$ is decomposed by N_c-point FFT into N_c frequency components:

$$R_{q,m}(k) = \sum_{t=0}^{N_c-1} r_{q,m}(t) \exp\left(-j2\pi t \frac{k}{N_c}\right). \tag{10}$$

Substituting Eq. (9) into Eq. (10), the k-th frequency component $R_{q,m}(k)$ of the q-th block is given by

$$R_{q,m}(k) = \sum_{n=0}^{N_t-1} H_{m,n}(k)\tilde{S}_{q,n}(k) + N_{q,m}(k), \tag{11}$$

where

$$\begin{cases} H_{m,n}(k) = \sum_{l=0}^{L-1} h_{m,n,l} \exp\left(-j2\pi k \frac{\tau_l}{N_c}\right) \\ N_{q,m}(k) = \sum_{t=0}^{N_c-1} \eta_{q,m}(t) \exp\left(-j2\pi k \frac{t}{N_c}\right) \end{cases}. \tag{12}$$

Frequency-domain STBC-JTRD decoding is carried out on $\{R_{q,m}(k);\ q{=}0{\sim}(Q-1),\ m{=}0{\sim}(N_r-1)\}$ as follows:

$$\hat{S}_0(k) = R_{0,0}(k) \quad \text{for } N_r = 1, \tag{13a}$$

$$\begin{pmatrix} \hat{S}_0(k) \\ \hat{S}_1(k) \end{pmatrix} = \begin{pmatrix} R_{0,0}(k) + R^*_{1,1}(k) \\ R_{0,1}(k) - R^*_{1,0}(k) \end{pmatrix} \quad \text{for } N_r = 2, \tag{13b}$$

$$\begin{pmatrix} \hat{S}_0(k) \\ \hat{S}_1(k) \\ \hat{S}_2(k) \end{pmatrix} = \begin{pmatrix} R_{0,0}(k) + R^*_{1,1}(k) + R^*_{2,2}(k) \\ R_{0,1}(k) - R^*_{1,0}(k) + R^*_{3,2}(k) \\ R_{0,2}(k) - R^*_{2,0}(k) - R^*_{3,1}(k) \end{pmatrix} \quad \text{for } N_r = 3, \tag{13c}$$

$$\begin{pmatrix} \hat{S}_0(k) \\ \hat{S}_1(k) \\ \hat{S}_2(k) \end{pmatrix} = \begin{pmatrix} R_{0,0}(k) + R^*_{1,1}(k) + R^*_{2,2}(k) + R_{3,3}(k) \\ R_{0,1}(k) - R^*_{1,0}(k) - R_{2,3}(k) + R^*_{3,2}(k) \\ R_{0,2}(k) + R_{1,3}(k) - R^*_{2,0}(k) - R^*_{3,1}(k) \end{pmatrix} \quad \text{for } N_r = 4. \tag{13d}$$

Then, N_c-point IFFT is applied to transform $\{\hat{S}_j(k);\ k{=}0{\sim}(N_c-1)\}$ into the time-domain signal block as

$$\hat{s}_j(t) = \frac{1}{N_c} \sum_{k=0}^{N_c-1} \hat{S}_j(k) \exp\left(j2\pi k \frac{t}{N_c}\right). \tag{14}$$

Finally, despreading is performed to get the decision variable $\hat{d}(i)$ for the i-th data symbol $d(i)$ as

$$\hat{d}(i) = \frac{1}{SF} \sum_{t=t_1}^{t_1+SF-1} \hat{s}_{\lfloor i/(N_c/SF)\rfloor}(t \bmod N_c)c^*(t), \tag{15}$$

based on which the data demodulation is carried out, where $t_1 = ((i \bmod (N_c/SF)) + (\lfloor i/(N_c/SF)\rfloor (N_c/SF))SF$.

3.3 Frequency-Domain STBC-JTRD Decoding without FFT/IFFT Operation

The frequency-domain STBC-JTRD decoding presented in Sect. 3.2 requires N_c-point FFT/IFFT operations to obtain $\{R_{q,m}(k)\}$ and transform them back to time-domain signal blocks. Below, an equivalent time-domain decoding that requires no FFT/IFFT operations is presented. N_c-point IFFT of $\{R^*_{q,m}(k);\ k{=}0{\sim}(N_c-1)\}$ can be expressed as

$$\frac{1}{N_c}\sum_{k=0}^{N_c-1} R^*_{q,m}(k)\exp\left(j2\pi k\frac{t}{N_c}\right) = r^*_{q,m}((N_c-t) \bmod N_c). \tag{16}$$

Hence, frequency-domain STBC-JTRD decoding of Eq. (13b) can be replaced by

$$\begin{pmatrix}\hat{s}_0(t)\\ \hat{s}_1(t)\end{pmatrix} = \begin{pmatrix} r_{0,0}(t)+r^*_{1,1}((N_c-t) \bmod N_c)\\ r_{0,1}(t)-r^*_{1,0}((N_c-t) \bmod N_c)\end{pmatrix} \text{ for } N_r = 2. \tag{17}$$

Equivalent time-domain decoding for N_r=1, 3 and 4 are omitted for the sake of brevity.

4. MMSE Pre-Equalization Weight

For the single-carrier transmission (including DS-CDMA) using pre-FDE, a good BER performance can be achieved by using the minimum mean square error (MMSE) weight that minimizes the mean square error (MSE) between the transmit signal and the received signal [9], [10]. In this paper, we will derive the MMSE weight for the frequency-domain STBC-JTRD. Since the frequency-domain STBC-JTRD encoding alters the transmitted signal spectrum shape in a frequency-selective fading channel, the signal-to-noise power ratio (SNR) is inproportional to the MSE [10]. Therefore, in this paper, we introduce the relative equalization error $e(k)$ defined as

$$e(k) = \frac{\hat{S}_0(k) - C_{N_r}\sqrt{2E_c/T_c}S_0(k)}{C_{N_r}\sqrt{2E_c/T_c}\sqrt{E[|S_0(k)|^2]}}. \tag{18}$$

Since the same data symbol is spread over all frequencies, the BER performance achievable with frequency-domain STBC-JTRD depends on the sum of the mean square relative equalization errors given as

$$e^2 = \sum_{k=0}^{N_c-1} E[|e(k)|^2]. \tag{19}$$

We can find the MMSE pre-equalization weight $w_{m,n}(k)$ that minimizes Eq. (19), i.e.,

$$\frac{\partial e^2}{\partial w_{m,n}(k)} = 0 \tag{20}$$

for all k=0∼(N_c-1), m=0∼(N_r-1) and n=0∼(N_t-1). After some manipulations, the following MMSE pre-equalization weight is obtained:

$$w_{m,n}(k) = \frac{H_{m,n}(k)}{\frac{1}{N_r}\bar{H}(k) + \left(\frac{1}{SF}\frac{E_s}{N_0}\right)^{-1}}, \tag{21}$$

where $E_s = E_c SF$ is the symbol energy and

$$\bar{H}(k) = \sum_{n=0}^{N_t-1}\sum_{m=0}^{N_r-1}|H_{m,n}(k)|^2. \tag{22}$$

5. BER Analysis

The conditional BER of DSSS using frequency-domain STBC-JTRD based on the Gaussian approximation of the inter-chip interference (ICI) is derived in a frequency-selective fading channel. Without loss of generality, we assume all "1" transmission and that the 0-th data symbol $d(0)$ is to be detected.

Substituting Eq. (13) into Eq. (14), $\hat{s}_0(t)$can be rewritten as

$$\hat{s}_0(t) = \frac{C_{N_r}}{N_c}\sqrt{\frac{2E_c}{T_c}}\left(\sum_{k=0}^{N_c-1}\hat{H}_{N_r}(k)\right)s_0(t) + \frac{C_{N_r}}{N_c}\sqrt{\frac{2E_c}{T_c}}\sum_{k=0}^{N_c-1}\hat{H}_{N_r}(k)\sum_{\substack{\tau=0\\ \tau\neq t}}^{N_c-1}s_0(\tau)\exp\left(j2\pi k\frac{t-\tau}{N_c}\right)+\hat{\eta}(t), \tag{23}$$

Where $\hat{H}_{N_r}(k)$ and $\hat{\eta}(t)$ respectively denote the equivalent channel gain and the noise, given by

$$\hat{H}_{N_r}(k) = \frac{\bar{H}(k)}{\frac{1}{N_r}\bar{H}(k) + \left(\frac{1}{SF}\frac{E_s}{N_0}\right)^{-1}}, \tag{24}$$

and

$$\hat{\eta}(t) = \begin{cases} \eta_{0,0}(t) + \eta^*_{1,1}((N_c-t) \bmod N_c), \text{ for} N_r = 2\\ \eta_{0,0}(t) + \eta^*_{1,1}((N_c-t) \bmod N_c)\\ \quad +\eta^*_{2,2}((N_c-t) \bmod N_c), \text{ for} N_r = 3\\ \eta_{0,0}(t) + \eta^*_{1,1}((N_c-t) \bmod N_c)\\ \quad +\eta^*_{2,2}((N_c-t) \bmod N_c) + \eta_{3,3}(t), \text{ for} N_r = 4 \end{cases}. \tag{25}$$

Substitution of Eq. (23) into Eq. (15) gives

$$\hat{d}(0) = C_{N_r}\sqrt{\frac{2E_c}{T_c}}\left(\frac{1}{N_c}\sum_{k=0}^{N_c-1}\hat{H}_{N_r}(k)\right)d(0) + \mu_{ICI} + \mu_{noise}, \tag{26}$$

where the first term represents the desired signal component and the second and third terms denote the ICI component and the noise component due to the AWGN, respectively. μ_{ICI} and μ_{noise} are given by

$$\mu_{ICI} = \frac{C_{N_r}}{SF \cdot N_c}\sqrt{\frac{2E_c}{T_c}}\sum_{t=0}^{SF-1}\sum_{k=0}^{N_c-1}\hat{H}_{N_r}(k) \times \sum_{\substack{\tau=0 \\ \tau\neq t}}^{N_c-1} s_0(\tau)\exp\left(j2\pi k\frac{t-\tau}{N_c}\right)c^*(t), \quad (27)$$

and

$$\mu_{noise} = \frac{1}{SF}\sum_{t=0}^{SF-1}\hat{\eta}(t)c^*(t). \quad (28)$$

It can be understood from Eq. (26) that the decision variable $\hat{d}(0)$ is a complex-valued random variable with mean $C_{N_r}\sqrt{\frac{2E_c}{T_c}}\left(\frac{1}{N_c}\sum_{k=0}^{N_c-1}\hat{H}_{N_r}(k)\right)d(0)$. Approximating μ_{ICI} as a zero-mean complex-valued Gaussian process, $\mu=\mu_{ICI} + \mu_{noise}$ can be treated as a new zero-mean complex-valued Gaussian noise. The variance $2\sigma_\mu^2$ of μ is the sum of those of μ_{ICI} and μ_{noise}. From Appendix A, we have

$$2\sigma_\mu^2 = 2\frac{N_c}{\sum_{n=0}^{N_t-1}\sum_{m=0}^{N_r-1}\sum_{k=0}^{N_c-1}|w_{m,n}(k)|^2}\frac{1}{SF} \times \frac{E_c}{T_c}\left[\frac{1}{N_c}\sum_{k=0}^{N_c-1}|\hat{H}_{N_r}(k)|^2 - \left|\frac{1}{N_c}\sum_{k=0}^{N_c-1}\hat{H}_{N_r}(k)\right|^2\right] + 2\frac{1}{SF}\frac{N_rN_0}{T_c}. \quad (29)$$

Since the ICI can be assumed to be circularly symmetric, the conditional BER for the given $\boldsymbol{H} = [H_{0,0}(0), H_{0,0}(1), \ldots, H_{0,0}(N_c - 1), \ldots, H_{N_r-1,N_t-1}(0), H_{N_r-1,N_t-1}(1), \ldots, H_{N_r-1,N_t-1}(N_c-1)]$ can be given by [2]

$$P_b\left(\frac{E_s}{N_0}, \boldsymbol{H}\right) = \frac{1}{2}\mathrm{erfc}\left[\sqrt{\frac{1}{4}\gamma_{N_r}\left(\frac{E_s}{N_0}, \boldsymbol{H}\right)}\right], \quad (30)$$

where $\mathrm{erfc}[x] = (2/\sqrt{\pi})\int_x^\infty \exp(-t^2)dt$ is the complementary error function. $\gamma_{N_r}(E_s/N_0, \boldsymbol{H})$ is the conditional signal-to-interference plus noise power ratio (SINR) and is given by

$$\gamma_{N_r}\left(\frac{E_s}{N_0}, \boldsymbol{H}\right) = \frac{2\frac{1}{N_r}\frac{E_s}{N_0}\left|\frac{1}{N_c}\sum_{k=0}^{N_c-1}\hat{H}_{N_r}(k)\right|^2}{\frac{1}{N_r}\frac{1}{SF}\frac{E_s}{N_0}\left[\frac{1}{N_c}\sum_{k=0}^{N_c-1}|\hat{H}_{N_r}(k)|^2 - \left|\frac{1}{N_c}\sum_{k=0}^{N_c-1}\hat{H}_{N_r}(k)\right|^2\right] + \frac{1}{N_c}\sum_{n=0}^{N_t-1}\sum_{m=0}^{N_r-1}\sum_{k=0}^{N_c-1}|w_{m,n}(k)|^2}, \quad (31)$$

where $\hat{H}_{N_r}(k)$ is given by Eq. (24).

The average BER can be numerically evaluated by averaging Eq. (30) over all the possible $\boldsymbol{H}$ as

$$P_b\left(\frac{E_s}{N_0}\right) = \underset{\boldsymbol{H}}{\mathrm{average}}\left[P_b\left(\frac{E_s}{N_0}, \boldsymbol{H}\right)\right]. \quad (32)$$

6. Numerical and Simulation Results

The numerical and simulation conditions are shown in Table 2. We assume N_c=256, N_g=32, and a chip-spaced L=16-path frequency-selective block Rayleigh fading channel with uniform power delay profile (i.e., the ensemble average of $E[|h_{m,n,l}|^2]$ is $1/L$ for all m, n, l). The ideal channel estimation for frequency-domain STBC-JTRD encoding is assumed. For comparison, we also evaluate, by computer simulation, the average BER performance of STTD with MMSE-FDE reception jointly used with MRC receive antenna diversity combining [14].

The numerical evaluation of the theoretical average BER performance is done by Monte-Carlo numerical computation method as follows. The set of path gains $\{h_{m,n,l}$; m=0~(N_r − 1), n=0~(N_t − 1) and l=0~(L − 1)$\}$ of an L-path Rayleigh fading channel is generated for obtaining $\{H_{m,n}(k)$; k=0~(N_c − 1)$\}$ using Eq. (12) and then $\{w_{m,n}(k)$; m=0~(N_r − 1), n=0~(N_t − 1) and k=0~(N_c − 1)$\}$ is computed using Eq. (21). The conditional BER for the given transmit E_s/N_0 and $\boldsymbol{H}$ is computed using Eq. (30). This is repeated a sufficient number of times to obtain the average BER $P_b(E_s/N_0)$ of Eq. (32).

The BER performance is also measured by computer simulation of the signal transmission. The computer simulation is carried out as follows. At the transmitter, a binary sequence is generated, QPSK data-modulated and then spread by a PN-sequence of 4095 chips. After an L=16-path Rayleigh fading channel is generated, the channel gains $\{H_{m,n}(k)$; k=0~(N_c − 1)$\}$ are computed using Eq. (12) and the pre-equalization weight $w_{m,n}(k)$ is computed using Eq. (21). Then, the frequency-domain STBC-JTRD encoded DSSS signal is generated by performing N_c-point IFFT (see Eq. (7)). At the receiver, after generating the received DSSS signal according to Eq. (9), the frequency-domain STBC-JTRD decoding is carried out in the time-domain as Eq. (17). Despreading is carried out to obtain the decision variables. The recovered binary sequence is compared with the transmitted binary sequence to measure the

Table 2 Numerical and simulation conditions.

Data modulation		QPSK
Transmitter	No. of FFT points	N_c=256
	Guard interval	N_g=32
	Spreading factor	SF=1, 16
	No. of transmit antennas	N_t=1, 2, 3, 4
	Pre-equalization weight	MMSE
Channel model	Fading type	Frequency-selective Rayleigh fading
	No. of paths	L=16
	Power delay profile	Uniform
	Time delay	$\tau_l=l$, l=0~L-1
Receiver	No. of receive antennas	N_r=1, 2, 3, 4
Channel estimation		Ideal

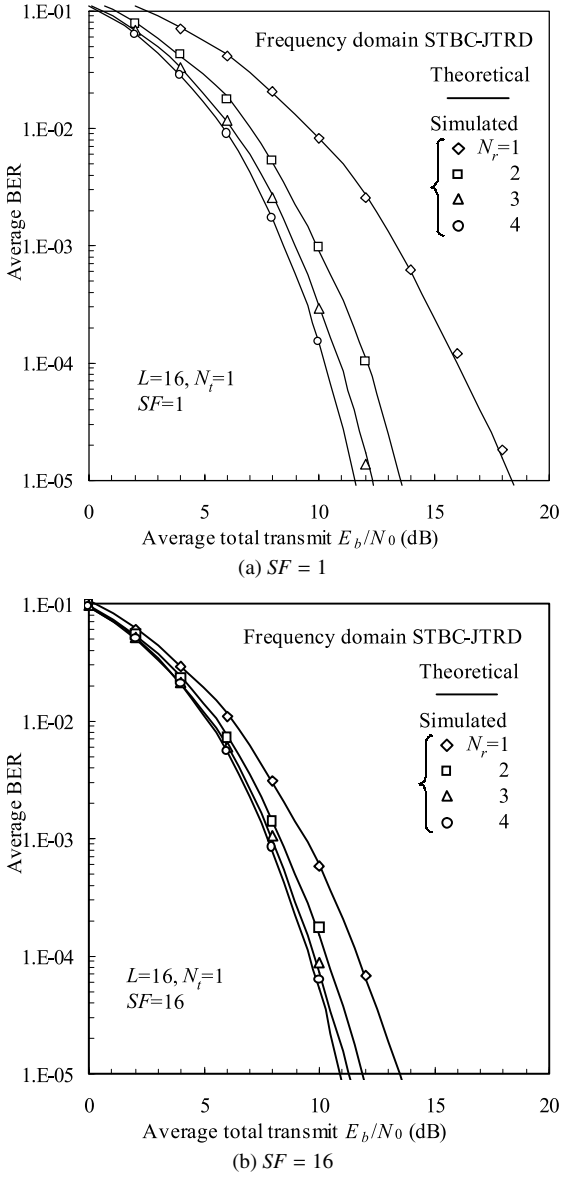

Fig. 3 Average BER performance with N_r as a parameter.

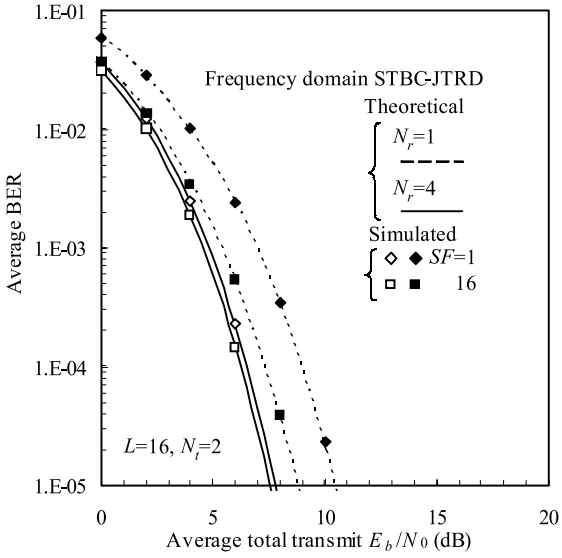

Fig. 4 Average BER performance with SF as a parameter.

number of bit errors. The above transmission and reception procedure is repeated a sufficient number of times to compute the average BER.

6.1 Average BER Performance of Frequency-Domain STBC-JTRD

Figure 3 shows the average BER performance achievable with frequency-domain STBC-JTRD as a function of the transmit E_b/N_0 (= $0.5(E_s/N_0)(1+N_g/N_c)$) with N_r and SF as parameters for N_t=1. It is seen from Fig. 3 that the BER performance is significantly improved by increasing N_r. When SF = 1, the required E_b/N_0 for BER=10^{-4} is reduced by 6 dB as N_r increases from 1 to 4, while it is reduced by 2 dB when SF = 16.

Figure 4 shows the BER performance of frequency-domain STBC-JTRD with SF as a parameter when N_t=2. As SF increases, the BER performance improves since the ICI can be better suppressed. However, the performance improvement by increasing the value of SF becomes less for N_r=4 receive antennas. The reduction of the required E_b/N_0 for obtaining BER=10^{-4} is 1.6 dB by increasing SF from 1 to 16 when N_r=1, but it is only 0.2 dB when N_r=4. This is because, for a large number of receiver antennas, the equivalent channel gain varies less in the frequency-domain (i.e., the channel becomes close to a frequency-nonselective channel), and hence the ICI can be sufficiently suppressed. In Figs. 3 and 4, a good agreement is seen between the theoretical and simulated results. This confirms our theoretical analysis based on the Gaussian approximation of the ICI.

6.2 Comparison of Frequency-Domain STBC-JTRD and Joint STTD&FDE Reception

Figure 5 compares the average BER performances of frequency-domain STBC-JTRD and joint STTD&FDE reception [14] (called frequency-domain STTD in this paper) with N_t as a parameter for SF = 1, 16. Figure 6 compares the average BER performances with N_r as a parameter. Similar to Sect. 5, we have derived the received SINR expression for DSSS using frequency-domain STTD, whose SINR is given by Eq. (31) but with N_r being replaced by N_t (its derivation is omitted for the sake of brevity).

It is seen from Fig. 5 that the performance improvement of frequency-domain STBC-JTRD by increasing N_t is larger than frequency-domain STTD, since the received SINR of STTD is reduced by a factor of $1/N_t$ than STBC-JTRD.

STBC-JTRD is compared with STTD [15]–[19] in Table 3. When N_t > 2, the coding-rate is reduced to R=3/4 for frequency-domain STTD, but it is kept as R=1 for frequency-domain STBC-JTRD. On the other hand, it can be seen from Fig. 6 that when N_r is increased, the BER per-

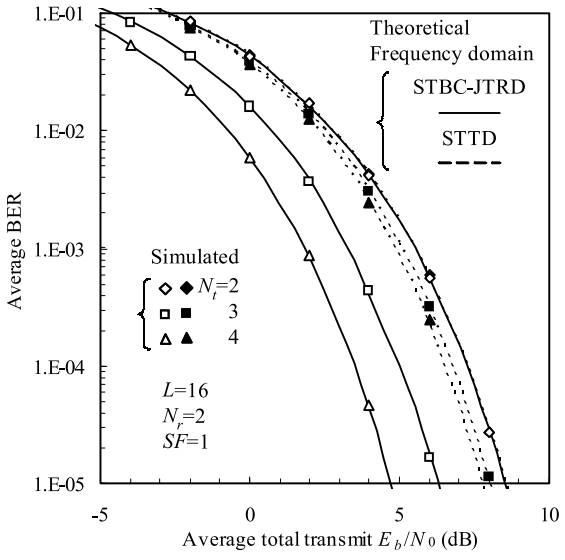

(a) SF = 1

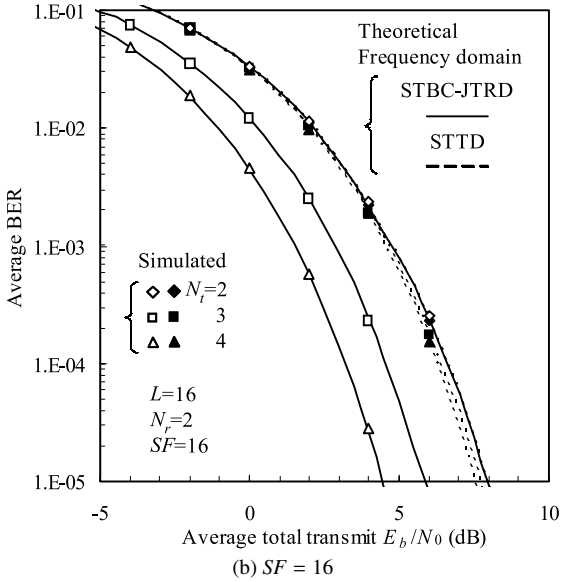

(b) SF = 16

Fig. 5 Comparison of frequency-domain STBC-JTRD and STTD with N_t as a parameter and N_r=2.

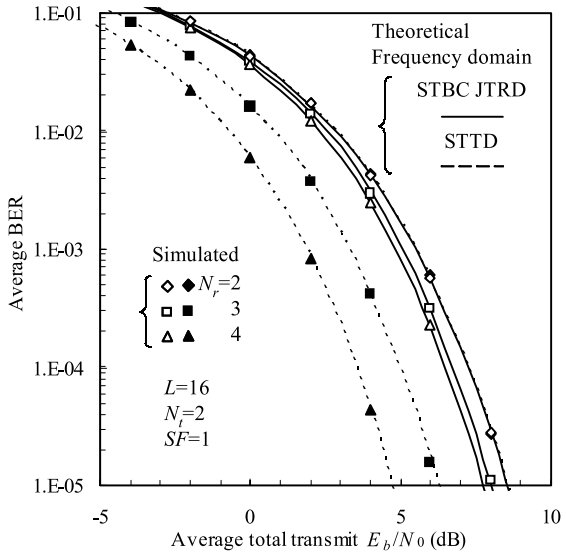

(a) SF = 1

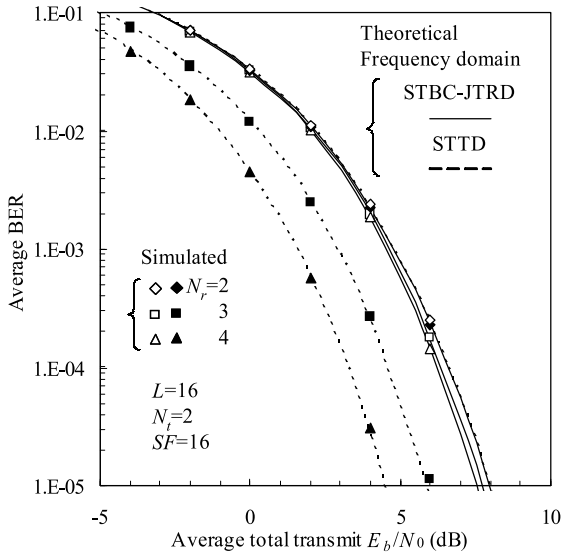

(b) SF = 16

Fig. 6 Comparison of frequency-domain STBC-JTRD and STTD with N_r as a parameter and N_t=2.

formance of frequency-domain STTD is significantly improved, while that of frequency-domain STBC-JTRD is only slightly improved. Therefore, the use of frequency-domain STBC-JTRD is advantageous for the downlink applications where the number of antennas at a mobile terminal is limited due to space limitation while a relatively large number of antennas can be implemented at a base station. Frequency-domain STTD is a good option for the uplink applications.

7. Conclusion

In this paper, we proposed the frequency-domain space-time block coded-joint transmit/receive diversity (frequency-domain STBC-JTRD) for DSSS signal transmission. Frequency-domain STBC-JTRD requires channel state in-

Table 3 Comparison of STBC-JTRD and STTD.

Diversity scheme	No. of transmit antennas, N_t	No. of receive antennas, N_r	CSI required at	Coding rate, R
STBC -JTRD [12, 13]	Arbitrary	2	Transmitter side	1
		3		3/4
		4		3/4
STTD [15-19]	2	Arbitrary	Receiver side	1
	3			3/4
	4			3/4
	5			2/3
	6			2/3
	7			5/8

formation (CSI) only at a transmitter side. The BER analysis was presented based on the Gaussian approximation of the inter-chip interference (ICI). The average BER performance was numerically evaluated and was confirmed by computer simulation. The performance comparison between frequency-domain STBC-JTRD and frequency-domain STTD showed that the BER performance improvement, by increasing the number of transmit antennas, is larger for frequency-domain STBC-JTRD than for frequency-domain STTD. In frequency-domain STBC-JTRD, an arbitrary number of transmit antennas can be used without reducing the coding rate when 2 receive antennas are used; however the coding rate reduces to 3/4 when 3 or 4 receive antennas are used. Frequency-domain STBC-JTRD is suitable for the downlink (base-to-mobile) applications since most of the antennas can be implemented at the base station for the given total number of antennas.

In this paper, we presented the frequency-domain STBC-JTRD coding of up to N_r=4 receive antennas. It is an open problem to find the frequency-domain STBC-JTRD with $N_r > 5$ receive antennas.

References

[1] W.C. Jakes, Jr., ed, Microwave Mobile Communications, Wiley, New York, 1974.
[2] J.G. Proakis, Digital Communications, 2nd ed., McGraw-Hill, 1995.
[3] Y. Akaiwa, Introduction to Digital Mobile Communication, Wiley, New York, 1997.
[4] D. Falconer, S.L. Ariyavisitakul, A. Benyamin-Seeyar, and B. Eidson, "Frequency domain equalization for single-carrier broadband wireless systems," IEEE Commun. Mag., vol.40, pp.58–66, April 2002.
[5] F. Adachi, M. Sawahashi, and H. Suda, "Wideband DS-CDMA for next-generation mobile communications systems," IEEE Commun. Mag., vol.36, pp.56–69, Sept. 1998.
[6] F. Adachi and K. Takeda, "Bit error rate analysis of DS-CDMA with joint frequency-domain equalization and antenna diversity combining," IEICE Trans. Commun., vol.E87-B, no.10, pp.2991–3002, Oct. 2004.
[7] I. Cosovic, M. Schnell, and A. Springer, "On the performance of different channel pre-compensation techniques for uplink time division duplex MC-CDMA," Proc. IEEE VTC'03 fall, vol.2, pp.857–861, Oct. 2003.
[8] S. Abe, S. Takaoka, H. Tomeba, and F. Adachi, "Frequency-domain pre-equalization for MC-CDMA/TDD uplink and its bit error rate analysis," IEICE Trans. Commun., vol.E89-B, no.1, pp.162–173, Jan. 2006.
[9] L.-U. Choi and R.D. Murch, "Frequency domain pre-equalization with transmit diversity for MISO broadband wireless communications," Proc. IEEE VTC'02 Fall, vol.3, pp.1784–1791, Oct. 2002.
[10] H. Tomeba, K. Takeda, and F. Adachi, "Frequency-domain pre-equalization for multi-code DS-CDMA mobile radio," Proc. IEEE VTS 2nd APWCS, pp.184–188, Aug. 2005.
[11] R. Esmailzadeh, M. Nakagawa, and A. Jones, "TDD-CDMA for the 4th generation of wireless communications," IEEE Wireless Commun., vol.10, no.4, pp.8–15, Aug. 2003.
[12] H. Tomeba, K. Takeda, and F. Adachi, "Space-time block coded transmit/receive diversity," IEEE VTC05 fall, vol.3, pp.2020–2024, Dallas, USA, Sept. 2005.
[13] H. Tomeba, K. Takeda, and F. Adachi, "Space-time block coded joint transmit/receive diversity in a frequency-nonselective Rayleigh fading channel," IEICE Trans. Commun., vol.E89-B, no.8, pp.2189–2195, Aug. 2006.
[14] K. Takeda and F. Adachi, "MMSE frequency-domain equalization combined with space-time transmit diversity and antenna received diversity for DS-CDMA," Proc. IEEE VTC'04 Spring, vol.1, pp.464–468, May 2004.
[15] S.M. Alamouti, "A simple transmit diversity technique for wireless communications," IEEE J. Sel. Areas. Commun., vol.16, no.8, pp.1451–1458, Oct. 1998.
[16] V. Tarokh, H. Jafarkhani, and A.R. Calderbank, "Space-time block coding for wireless communications: Performance results," IEEE J. Sel. Areas Commun., vol.17, no.3, pp.451–460, March 1999.
[17] V. Tarokh, H. Jafarkhani, and A.R. Calderbank, "Space-time block codes from orthogonal designs," IEEE Trans. Inf. Theory, vol.45, no.5, pp.1456–1467, July 1999.
[18] X.-B. Liang, "A high-rate orthogonal space-time block code," IEEE Commun. Lett., vol.7, no.5, pp.222–223, May 2003.
[19] W. Su, X.G. Xia, and K.J. R Liu, "A systematic design of high-rate complex orthogonal space-time block codes," IEEE Commun. Lett., vol.8, no.6, pp.380–382, June 2004.

Appendix A: Derivation of $2\sigma^2_{ICI}$ and $2\sigma^2_{noise}$ of Frequency-Domain STBC-JTRD in DSSS

First, we obtain $2\sigma^2_{ICI}$. From Eq. (27), the variance $2\sigma^2_{ICI}$ of μ_{ICI} can be given by

$$\begin{aligned}2\sigma^2_{\mu_{ICI}} &= E[|\mu_{ICI}|^2] = \frac{C^2_{N_r}}{SF^2N_c^2}\frac{2E_c}{T_c}\\ &\times \sum_{t=0}^{SF-1}\sum_{t'=0}^{SF-1}\sum_{k=0}^{N_c-1}\sum_{k'=0}^{N_c-1}\hat{H}(k)\hat{H}(k')\sum_{\substack{\tau=0\\ \tau\neq t}}^{N_c-1}\sum_{\substack{\tau'=0\\ \tau'\neq t'}}^{N_c-1}\\ &\times\left[\begin{array}{l} E[s_0(\tau)s_0^*(\tau')c^*(t)c(t')]\\ \times\exp\left(j2\pi k\frac{t-\tau}{N_c}\right)\exp\left(-j2\pi k'\frac{t'-\tau'}{N_c}\right)\end{array}\right]. \qquad (A\cdot 1)\end{aligned}$$

The DSSS signal $s(t)$ is white-noise like and hence, $E[s(\tau)s^*(\tau')c^*(t)c(t')] = \delta(\tau-\tau')\delta(t-t')$. we have

$$\begin{aligned}2\sigma^2_{\mu_{ICI}} &= \frac{N_c}{\sum_{n=0}^{N_t-1}\sum_{m=0}^{N_r-1}\sum_{k=0}^{N_c-1}|w_{m,n}(k)|^2}\frac{1}{SF^2N_c^2}\frac{2E_c}{T_c}\\ &\times\sum_{t=0}^{SF-1}\sum_{t'=0}^{SF-1}\sum_{k=0}^{N_c-1}\sum_{k'=0}^{N_c-1}\hat{H}(k)\hat{H}(k')\\ &\times\sum_{\substack{\tau=0\\ \tau\neq t}}^{N_c-1}\sum_{\substack{\tau'=0\\ \tau'\neq t'}}^{N_c-1}\left[\begin{array}{l}\delta(t-t')\delta(\tau-\tau')\\ \times\exp\left(j2\pi k\frac{t-\tau}{N_c}\right)\exp\left(-j2\pi k'\frac{t'-\tau'}{N_c}\right)\end{array}\right]\\ &= \frac{N_c}{\sum_{n=0}^{N_t-1}\sum_{m=0}^{N_r-1}\sum_{k=0}^{N_c-1}|w_{m,n}(k)|^2}\frac{1}{SF^2N_c^2}\frac{2E_c}{T_c}\\ &\times\sum_{t=0}^{SF-1}\sum_{k=0}^{N_c-1}\sum_{k'=0}^{N_c-1}\hat{H}(k)\hat{H}(k')\\ &\times\left[\sum_{\tau=0}^{N_c-1}\exp\left(j2\pi(k-k')\frac{t-\tau}{N_c}\right)-1\right]. \qquad (A\cdot 2)\end{aligned}$$

Since $\sum_{\tau=0}^{N_c-1} \exp\left(j2\pi(k-k')\frac{t-\tau}{N_c}\right) = N_c\delta(k-k')$, we obtain

$$\begin{aligned}
2\sigma_{ICI}^2 &= \frac{N_c}{\sum_{n=0}^{N_t-1}\sum_{m=0}^{N_r-1}\sum_{k=0}^{N_c-1}|w_{m,n}(k)|^2}\frac{1}{SF^2N_c^2}\frac{2E_c}{T_c} \\
&\quad\times\sum_{t=0}^{SF-1}\sum_{k=0}^{N_c-1}\sum_{k'=0}^{N_c-1}\hat{H}(k)\hat{H}^*(k')\left[N_c\delta(k-k')-1\right] \\
&= \frac{N_c}{\sum_{n=0}^{N_t-1}\sum_{m=0}^{N_r-1}\sum_{k=0}^{N_c-1}|w_{m,n}(k)|^2}\frac{1}{SFN_c^2}\frac{2E_c}{T_c} \\
&\quad\times\left[\begin{array}{l} N_c\displaystyle\sum_{k=0}^{N_c-1}\sum_{k'=0}^{N_c-1}\hat{H}(k)\hat{H}^*(k')\delta(k-k') \\ -\displaystyle\sum_{k=0}^{N_c-1}\sum_{k'=0}^{N_c-1}\hat{H}(k)\hat{H}^*(k')\end{array}\right] \\
&= 2\frac{N_c}{\sum_{n=0}^{N_t-1}\sum_{m=0}^{N_r-1}\sum_{k=0}^{N_c-1}|w_{m,n}(k)|^2}\frac{1}{SF}\frac{E_c}{T_c} \\
&\quad\times\left[\begin{array}{l}\dfrac{1}{N_c}\displaystyle\sum_{k=0}^{N_c-1}|\hat{H}(k)|^2 \\ -\left|\dfrac{1}{N_c}\displaystyle\sum_{k=0}^{N_c-1}\hat{H}(k)\right|^2\end{array}\right]. \qquad (A\cdot 3)
\end{aligned}$$

Next, we obtain $2\sigma_{noise}^2$. Using Eq. (28), the noise variance $2\sigma_{noise}^2$ is obtained from

$$\begin{aligned}
2\sigma_{noise}^2 &= E[|\mu_{noise}|^2] \\
&= \frac{1}{SF^2}\sum_{t=0}^{SF-1}\sum_{t'=0}^{SF-1}E[\eta(t)\eta^*(t')c^*(t)c(t')]. \qquad (A\cdot 4)
\end{aligned}$$

Since $E[c^*(t)c(t')] = \delta(t-t')$, we have

$$2\sigma_{noise}^2 = \frac{1}{SF^2}\sum_{t=0}^{SF-1}E[|\eta(t)|^2] = 2\frac{1}{SF}\frac{N_rN_0}{T_c}. \qquad (A\cdot 5)$$

Appendix B: Relationship between Frequency-Domain STBC-JTRD and STTD

For frequency-domain STTD with N_t=4 transmit antennas and N_r=1 receive antenna, the k-th frequency component $\{R_{q,0}(k);\ q=0\sim3\}$ of the q-th received signal block is given by

$$\begin{pmatrix} R_{0,0}(k) \\ R_{1,0}(k) \\ R_{2,0}(k) \\ R_{3,0}(k)\end{pmatrix} = \mathrm{diag}\left[\boldsymbol{S}(k)\boldsymbol{H}(k)\right], \qquad (A\cdot 6)$$

where $\boldsymbol{S}(k)$ and $\boldsymbol{H}(k)$ are given by [13], [14]

$$\boldsymbol{S}(k) = \begin{pmatrix} S_0(k) & S_1(k) & S_2(k) \\ S_0^*(k) & S_1^*(k) & S_2(k) \\ S_0^*(k) & S_1(k) & S_2^*(k) \\ S_0(k) & S_1^*(k) & S_2^*(k)\end{pmatrix}, \qquad (A\cdot 7)$$

$$\boldsymbol{H}(k) = \begin{pmatrix} H_{0,0}(k) & H_{0,1}(k) & H_{0,2}(k) & H_{0,3}(k) \\ H_{0,1}(k) & -H_{0,0}(k) & -H_{0,3}(k) & H_{0,2}(k) \\ H_{0,2}(k) & H_{0,3}(k) & -H_{0,0}(k) & -H_{0,1}(k)\end{pmatrix}. \qquad (A\cdot 8)$$

Frequency-domain STTD decoding is carried out as

$$\begin{pmatrix} \hat{S}_0(k) \\ \hat{S}_1(k) \\ \hat{S}_2(k)\end{pmatrix} = \mathrm{diag}\left[\boldsymbol{W}(k)\boldsymbol{R}(k)\right], \qquad (A\cdot 9)$$

where

$$\boldsymbol{W}(k) = \begin{pmatrix} w_{0,0}^*(k) & w_{0,1}(k) & w_{0,2}(k) & w_{0,3}^*(k) \\ w_{0,1}^*(k) & -w_{0,0}(k) & -w_{0,3}^*(k) & w_{0,2}(k) \\ w_{0,2}^*(k) & w_{0,3}^*(k) & -w_{0,0}(k) & -w_{0,1}(k)\end{pmatrix}, \qquad (A\cdot 10)$$

$$\boldsymbol{R}(k) = \begin{pmatrix} R_{0,0}(k) & R_{0,0}(k) & R_{0,0}(k) \\ R_{1,0}^*(k) & R_{1,0}^*(k) & R_{1,0}(k) \\ R_{2,0}^*(k) & R_{2,0}(k) & R_{2,0}^*(k) \\ R_{3,0}(k) & R_{3,0}^*(k) & R_{3,0}^*(k)\end{pmatrix}. \qquad (A\cdot 11)$$

In this paper, $\boldsymbol{W}(k)$ is called the frequency-domain STTD decoding matrix.

On the other hand, frequency-domain STBC-JTRD encoding (see Eq. (5d)) with N_t=1 transmit antenna and N_r=4 receive antennas can be rewritten as

$$\begin{pmatrix} \tilde{S}_{0,0}(k) \\ \tilde{S}_{1,0}(k) \\ \tilde{S}_{2,0}(k) \\ \tilde{S}_{3,0}(k)\end{pmatrix} = \mathrm{diag}[\hat{\boldsymbol{W}}^T(k)\boldsymbol{S}^T(k)], \qquad (A\cdot 12)$$

where $\hat{\boldsymbol{W}}(k)$ can be expressed as

$$\hat{\boldsymbol{W}}(k) = \begin{pmatrix} w_{0,0}^*(k) & w_{1,0}^*(k) & w_{2,0}^*(k) & w_{3,0}^*(k) \\ w_{1,0}^*(k) & -w_{0,0}^*(k) & -w_{3,0}^*(k) & w_{2,0}^*(k) \\ w_{2,0}^*(k) & w_{3,0}^*(k) & -w_{0,0}^*(k) & -w_{1,0}^*(k)\end{pmatrix}. \qquad (A\cdot 13)$$

It can be understood from Eqs. (A· 10), (A· 12) and (A· 13) that the frequency-domain STBC-JTRD encoding is carried out by using the frequency-domain STTD decoding matrix $\boldsymbol{W}(k)$ but with $\{w_{0,n}(k);\ n=0\sim3\}$ being replaced by $\{w_{m,0}^*(k);\ m=0\sim3\}$ as the encoding matrix $\hat{\boldsymbol{W}}(k)$.

On the other hand, frequency-domain STBC-JTRD decoding can be carried out by the same addition/subtraction and conjugate operations as Eq. (A· 9) but with $\{R_{q,0}(k)w_{0,m}(k);\ q=0\sim3,\ m=0\sim3\}$ being replaced by the received signal $\{R_{q,m}(k);\ q=0\sim3,\ m=0\sim3\}$ of the frequency-domain STBC-JTRD.

Hiromichi Tomeba received his B.S. and M.S. degrees in communications engineering from Tohoku University, Sendai, Japan, in 2004 and 2006. Currently he is a Japan Society for the Promotion of Science (JSPS) research fellow, studying toward his PhD degree at the Department of Electrical and Communications Engineering, Graduate School of Engineering, Tohoku University. His research interests include frequency-domain equalization and antenna diversity techniques for mobile communication systems. He was a recipient of the 2004 and 2005 IEICE RCS (Radio Communication Systems) Active Research Award.

Kazuaki Takeda received his B.E. and M.S. degrees in communications engineering from Tohoku University, Sendai, Japan, in 2003 and 2004. Currently he is a Japan Society for the Promotion of Science (JSPS) research fellow, studying toward his Ph.D. degree at the Department of Electrical and Communications Engineering, Graduate School of Engineering, Tohoku University. His research interests include equalization, interference cancellation, transmit/receive diversity, and multiple access techniques. He was a recipient of the 2003 IEICE RCS (Radio Communication Systems) Active Research Award and 2004 Inose Scientific Encouragement Prize.

Fumiyuki Adachi received the B.S. and Dr. Eng. degrees in electrical engineering from Tohoku University, Sendai, Japan, in 1973 and 1984, respectively. In April 1973, he joined the Electrical Communications Laboratories of Nippon Telegraph & Telephone Corporation (now NTT) and conducted various types of research related to digital cellular mobile communications. From July 1992 to December 1999, he was with NTT Mobile Communications Network, Inc. (now NTT DoCoMo, Inc.), where he led a research group on wideband/broadband CDMA wireless access for IMT-2000 and beyond. Since January 2000, he has been with Tohoku University, Sendai, Japan, where he is a Professor of Electrical and Communication Engineering at the Graduate School of Engineering. His research interests are in CDMA wireless access techniques, equalization, transmit/receive antenna diversity, MIMO, adaptive transmission, and channel coding, with particular application to broadband wireless communications systems. From October 1984 to September 1985, he was a United Kingdom SERC Visiting Research Fellow in the Department of Electrical Engineering and Electronics at Liverpool University. He was a co-recipient of the IEICE Transactions best paper of the year award 1996 and again 1998 and also a recipient of Achievement award 2003. He is an IEEE Fellow and was a co-recipient of the IEEE Vehicular Technology Transactions best paper of the year award 1980 and again 1990 and also a recipient of Avant Garde award 2000. He was a recipient of Thomson Scientific Research Front Award 2004.